

Synthesis of boron nitride nanotubes by means of excimer laser ablation at high temperature

D. P. Yu,^{a)} X. S. Sun, C. S. Lee,^{b)} I. Bello, S. T. Lee, H. D. Gu, and K. M. Leung
Department of Physics & Material Science, City University of Hong Kong, Kowloon, Hong Kong

G. W. Zhou, Z. F. Dong, and Z. Zhang
Beijing Lab of Electron Microscopy, Academia Sinica, 100080 Beijing, People's Republic of China

(Received 26 September 1997; accepted for publication 13 February 1998)

Boron nitride nanotubes (BN-NTs) were synthesized by using excimer laser ablation at 1200 °C in different carrier gases. The main characteristic of the BN-NTs produced by this method is that nanotubes are of only one to three atomic layers thick, which could be attributed to the dominance of the axial growth rate over the radial growth rate. The diameter of the BN-NTs ranged from 1.5 to 8 nm. The tips of the BN-NTs are either a flat cap or of polygonal termination, in contrast to the conical ends of carbon nanotubes. The atomic ratio of boron to nitrogen as measured by means of parallel electron energy loss spectroscopy is 0.8, which is within the experimental error of the stoichiometry of hexagonal BN structure. © 1998 American Institute of Physics.
[S0003-6951(98)00816-X]

The discovery of carbon nanotubes (CNTs) has motivated intense interest in the study of their peculiar structure, physical properties, and potential technological applications.^{1,2} Based on the analogy between graphite carbon sheet and hexagonal boron nitride (BN) as well as BCN structures, it was theoretically predicted that wrapping the hexagonal BN and BCN sheets can respectively produce BN and BCN nanotubes which should be more energetically favorable. Theoretical calculation reveals that the electrical properties of CNTs may range from metallic to semiconducting behavior, strongly depending on the chirality and diameter of the nanotube. It is also predicted that boron nitride nanotubes (BN-NTs) have a semiconducting property with nearly constant band gap, which is independent of the structure of the nanotubes.^{3,4} Therefore, BN-NTs may provide a very interesting possibility for potential application for devices. BN-NTs and BCN nanotubes had been fabricated by different groups,⁵⁻⁹ all by means of the arc-discharge method. However, oven-excimer laser ablation technique has recently turned out to be a powerful means for the synthesis of CNTs. It gives CNTs not only with perfect structure and high yield, but also with single atomic layer and a uniform diameter of about 1.4 nm.^{10,11} Single-walled nanotubes are of scientific importance because they make the study of their intrinsic physical properties possible and easier. Comparing with the arc-discharge method, the oven-laser ablation process has the advantage that diverse growth parameters, such as the wavelength and the energy density of the laser beam, the pressure and flow rate of carrier gases, the growth temperature, the kind of target materials and so on, can be easily controlled. No report has yet been published on the synthesis of BN-NTs using laser ablation, especially single-walled BN-NTs. In this letter, we will report on the production of BN-NTs by means of excimer laser ablation at high tempera-

ture and the influence of various atmospheres on the morphology of BN-NTs. The BN-NTs so produced were predominantly one to three atomic layers thick.

The oven-laser ablation method that we used in this study is similar to that used for the synthesis of single-walled CNTs.¹¹ The target material was prepared by mixing BN powder (99.5% in purity) with nanosized Ni and Co powder (1 at% each). The mixed powder was hot pressed at 150 °C to form a plate target. The laser we used was an excimer laser (Lambda Physik, LEXtra 200) with a wavelength of 248 nm. The target was placed inside a ϕ 42 mm \times 750 mm long quartz tube heated by a tube furnace. The quartz tube was firstly evacuated to about 20 mTorr, then filled with flowing carrier gases including argon, nitrogen, or helium at a flow rate of 100 sccm. After about 20 h of degassing at 1200 °C, the laser beam was focused into a spot of 1 \times 3 mm² on the target, and the target was ablated at 1200 °C. The frequency of the laser beam was 10 Hz (pulse duration=34 ns) and the average energy per pulse was about 400 mJ. The ablated materials were carried by the flowing carrier gas, and were collected on the water-cooled copper collector mounted downstream inside the quartz tube.

Light gray powder was deposited on the copper collector. Samples destined for transmission electron microscopy analysis was prepared by ultrasonic dispersion of the collected powder in ethanol. A drop of the suspension solution was placed on a holey carbon film grid. High resolution electron microscopy (HREM) was conducted by using a Jeol-2010 microscope with a point-to-point resolution of about 0.19 nm. Electron-energy loss spectroscopic analysis for the bonding state and chemical composition of the BN-NTs was made by using a Philips-CM200 FEG microscope equipped with a Gatan parallel electron energy loss spectrometer (PEELs). Raman spectrum was obtained by using a Renishaw 2000 system with a laser source of 514.5 nm.

A representative micrograph showing the general view of the morphology of the BN-NTs obtained in a argon atmosphere is shown in Fig. 1(a). Abundant pure BN-NTs are

^{a)}On leave from Department of Physics, Peking University, 100871 Beijing, People's Republic of China.

^{b)}Corresponding author. Electronic mail: APCSLLEE@cityu.edu.hk

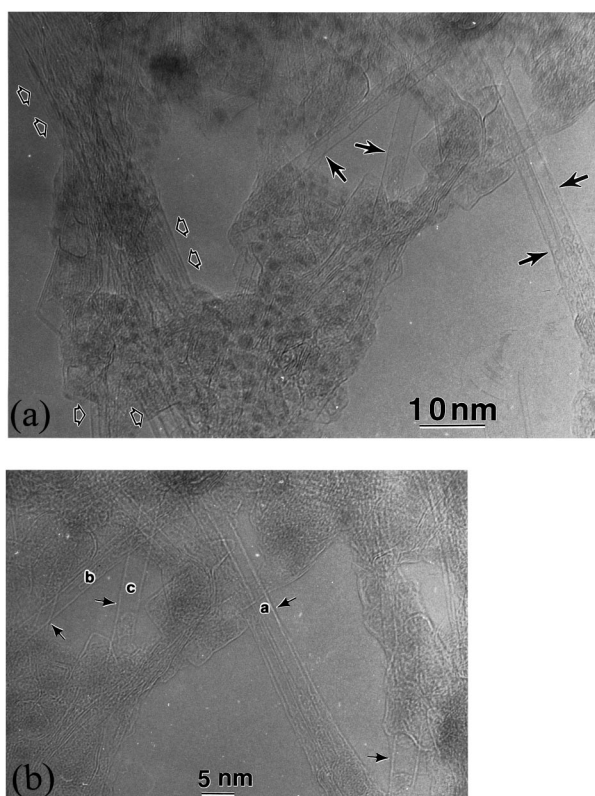
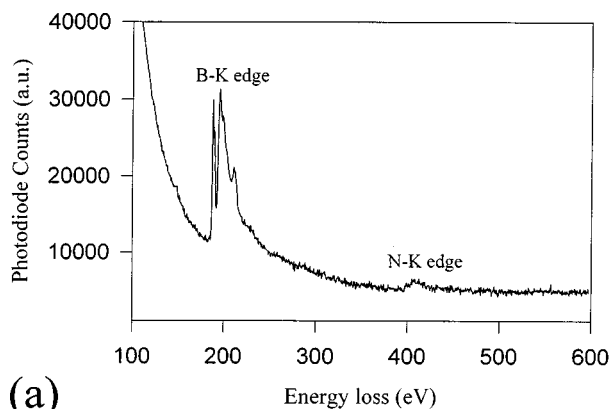
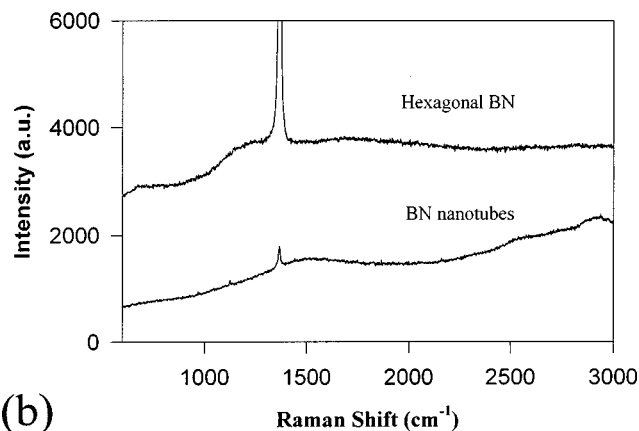


FIG. 1. (a) A typical HREM micrograph showing a general view of the BN-NTs grown in flowing Ar carrier gas. Abundant BN-NTs are visible. They appear either as individual tubes (indicated with black arrows), or as bundles (marked with hollow arrows). The main characteristic feature is that single-walled BN-NTs are dominant. Nanosized metallic particles with dark contrast are found embedded in the amorphous matrix. (b) A representative HREM image revealing the dominant single-walled BN-NTs (marked with black arrows). The diameter of tubes labeled *a*, *b*, and *c* is 2.1, 2.2, and 3 nm, respectively. The outer surface of the BN-NTs is clean, without any attachment of amorphous materials. No encapsulation of metallic particles was observed inside the nanotubes.

visible in the image. The BN-NTs appear either as individual tubes indicated by solid arrows, or as bundles running from bottom towards upper left of the image marked with hollow arrows. We estimated that the yield of the BN-NTs synthesized in an argon atmosphere could be as high as 40% of the ablated materials. A magnified portion of the image is shown in Fig. 1(b). The main characteristics of the BN-NTs in Fig. 1(b) is that most BN-NTs are single walled. The diameters of tubes labeled ‘‘*a*,’’ ‘‘*b*,’’ and ‘‘*c*’’ are 2.1, 2.2, and 3 nm, respectively. (Diameters of the nanotubes were measured directly from the negative film taken at the Gaussian focusing condition. The overfocused image, Fig. 1(b), is shown here for its better contrast.) Unlike the uniform diameter of single-walled CNTs synthesized by similar method,⁸ the diameters of the present BN-NTs are variable from 1.5 to 8 nm, with a sharp population peak at about 2.2 nm. The outer surface of the single layered BN-NTs is very clean, without any attachment of amorphous coating. Nanosized particles with dark contrast are visible in the image. These are clusters of Co and Ni catalysts embedded in the amorphous matrix. Their diameter ranges from 0.5 to 4 nm. No encapsulation of the Co–Ni catalyst particles was observed inside the nanotubes, as it was the case of BN-NTs grown by the arc-discharge method.⁵



(a)



(b)

FIG. 2. (a) PEELS spectrum taken from an individual BN-NT. The distinct absorption features at 188 and 401 eV correspond to the known *B–K* edge and *N–K* edge, respectively. (b) Comparison of Raman spectra of hexagonal BN powder and the powder product containing abundant BN-NTs. The distinct Raman shift onset at about 1367 cm^{-1} confirms the layered graphitic structure of the BN-NTs.

The bonding state and chemical composition of the BN-NTs were determined by PEELS. The spectrum shown in Fig. 2(a) was taken from an individual BN-NTs suspended over the hole of the supporting holey carbon film grid. The spot size of the electron probe is about 2 nm in diameter. Two distinct absorption features are visible in the spectrum, one starting at 188 eV and another at 401 eV, corresponding to the known *B–K* edge and *N–K* edge, respectively. Analysis of the PEELS spectrum gives a B:N ratio of about 0.8. This value, with consideration of the experimental error of about 20% due mainly to background subtraction, is consistent with the stoichiometric B:N ratio in hexagonal BN.

Figure 2(b) shows a comparison of the Raman spectra of the hexagonal BN powder and the powder product containing BN-NTs. A small, but distinct Raman shift at about 1367 cm^{-1} confirms a layered graphitic structure of the BN-NTs.

Comparison of the structure of the BN-NTs synthesized with different carrier gases reveals an interesting phenomenon. BN-NTs obtained in inert carrier gases such as argon and helium, were dominated with a one-layer structure (Fig. 1). When nitrogen was used as the carrier gas, the BN-NTs were dominated with tubes of two layers (Fig. 3). No BN-NTs with more than four layers were observed. The interplanar spacing between two layers is about 0.33 nm, which is consistent with the interplanar distance in bulk hexagonal

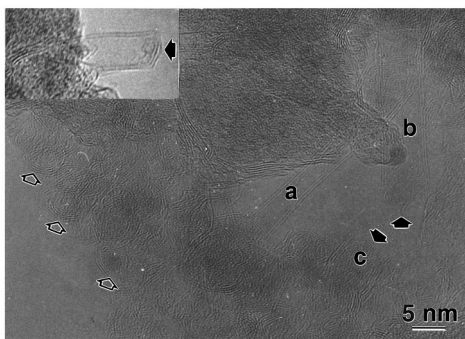


FIG. 3. HREM image of BN-NTs grown in N_2 atmosphere. Two-layered BN-NTs are visible. The tube labeled *c* and the tube shown in inset have peculiar flat tips (indicated with solid arrows). The tube labeled with *b* have a blur and polygonal end which is not completely closed. Many “onion-like” structures, are visible at the lower-left part of the image, as indicated with short hollow arrows. Some metallic particles are enclosed inside the onion.

BN. The two-layered BN-NTs labeled with *a* and *b* in Fig. 3 have a diameter of 4 and 7.7 nm, respectively. In general, the diameter of the BN-NTs produced under a nitrogen environment is larger than that produced under an inert gas environment. One of the possible causes is probably that the size and charge of the atoms of the carrier gas may significantly influence the mean-free path or lifetime of the activated B and N species knocked out by the laser from the target, and thus affect the growth of the BN-NTs. There are a lot of onionlike structures visible in the lower-left part of Fig. 3 (marked with arrows). These BN “onions” are not completely closed, and metallic particles are enclosed inside.

While most of the BN-NTs observed here have their tip embedded in the amorphous matrix, some tips are occasionally visible and reveal dramatic morphological difference in comparison to that of CNTs. A typical example is shown in Fig. 3. The BN-NT labeled *c* has a peculiar platelike tip perpendicular to the tube axis (marked with short solid arrow). The tip morphology of the BN-NT in the inset has a similar configuration. The end of the BN-NT labeled *b* has a blur, but polygonal contrast, and is not closed completely. Dense metallic particles have been found inside the BN-NTs ends,⁵ but there is no evidence of such a termination of BN-NTs in the present investigation. Flat tips of BN-NTs have also been observed by another group, and it was explained as a combination of three disclinations.⁶ Polygonal ends were observed in BN-NTs produced by laser heating at high pressure.¹² These peculiar tip morphologies are different from those of CNTs which usually have smooth conical caps.^{13,14} The formation of the conical tips needs to introduce pentagons.¹³ In the BN system, however, introduction of pentagons into the graphitic network will unavoidably cause B–B and N–N bondings, which is energetically unfavorable.⁵ It seems that flat and polygonal capping is a characteristic feature of BN-NTs because of its high ionicity.

Though BN-NTs have been synthesized successfully by arc discharge as well as by the present method, the mecha-

nism for their formation is still obscure, and the role of the metallic catalysts remains an open question. In catalytic growth of CNTs, metal catalyst particles were frequently observed encapsulated inside the nanotubes, either in the middle or at the cap part of nanotubes. It is therefore suggested that the catalyst particles act as a carbon transporter, and as a nucleation site where the CNTs can grow. In our experiments, the nanosized catalyst particles, visible as spots of dark contrast in Fig. 1(a), are not encapsulated inside the BN-NTs. Instead they are embedded in the amorphous matrix, indicating that the catalyst atoms may play an important part in the gas atmosphere during the growth of BN-NTs. The metallic atoms may help to keep the dangling bonds open, and prevent the formation of closed onion structure, so that the forthcoming B and N atoms may chemisorb on the growing sites to continue the hexagonal network. The competition between axial and radial growth determines whether the nanotubes is multiwalled or single walled. In the present case, the axial growth rate is probably much greater than the radial growth, so that BN-NTs of single wall, or having only a few layers, are formed.

In conclusion, BN-NTs have been synthesized by means of excimer laser ablation at 1200 °C. The BN-NTs produced are single layered or only a few layers, which are believed to be due to the higher axial growth rate in comparison to the radial growth rate. The BN-NTs have a flat or polygonal tip structure, which is different from the conical ends of carbon nanotubes.

The financial support of Research Grant Council of Hong Kong Government and of City University of Hong Kong via Strategic Research Grants is gratefully acknowledged.

¹S. Iijima, *Nature (London)* **354**, 56 (1991).

²V. Ivanov, J. B. Nagy, Ph. Lambin, A. Lucas, X. B. Zhang, X. F. Zhang, D. Bernaerts, G. Van Tendeloo, S. Amelinkx, and J. Van Landuyt, *Chem. Phys. Lett.* **223**, 329 (1994).

³A. Rubio, J. L. Corkill, and M. L. Cohen, *Phys. Rev. B* **49**, 5081 (1994).

⁴Y. Miyamoto, A. Rubio, M. L. Cohen, and S. G. Louie, *Phys. Rev. B* **50**, 4976 (1994).

⁵N. G. Chopra, R. J. Luyken, K. Cherrey, V. H. Crespi, M. L. Cohen, S. G. Louie, and A. Zettl, *Science* **269**, 966 (1995).

⁶A. Loiseau, F. Williaime, N. Demoncey, G. Hug, and H. Pascard, *Phys. Rev. Lett.* **76**, 4737 (1996).

⁷O. Stephan, P. M. Ajayan, C. Colliex, Ph. Redlich, J. M. Lambert, P. Bernier, and P. Lefin, *Science* **266**, 1683 (1994).

⁸Z. Weng-Sieh, K. Cherrey, N. G. Chopra, X. Blase, Y. Miyamoto, A. Rubio, M. L. Cohen, S. G. Louie, A. Zettl, and R. Gronsky, *Phys. Rev. B* **51**, 11 229 (1995).

⁹Ph. Redlich, J. Loeffler, P. M. Ajayan, J. Bill, F. Aldinger, and M. Rühler, *Chem. Phys. Lett.* **260**, 465 (1996).

¹⁰T. Guo, P. Nikolaev, A. Thess, D. T. Colbert, and R. E. Smalley, *Chem. Phys. Lett.* **243**, 49 (1995).

¹¹A. Thess, R. Lee, P. Nikolaev, H. Dai, P. Petit, J. Robert, C. Xu, Y. H. Lee, S. G. Kim, A. G. Rinzler, D. T. Colbert, G. E. Scuseria, D. Tomaneck, J. E. Fischer, and R. E. Smalley, *Science* **273**, 483 (1996).

¹²D. Golberg, Y. Bando, M. Eremets, K. Takemura, K. Kurashima, and H. Yusa, *Appl. Phys. Lett.* **69**, 2045 (1996).

¹³S. Iijima, T. Ichihashi, and Y. Ando, *Nature (London)* **356**, 776 (1992).

¹⁴S. Iijima, *Mater. Sci. Eng. B* **19**, 172 (1993).